

## Structural and Functional Insights into Sulfide:Quinone Oxidoreductase<sup>†,‡</sup>

José A. Brito,<sup>§,||</sup> Filipa L. Sousa,<sup>§,||</sup> Meike Stelter,<sup>§,#</sup> Tiago M. Bandeiras,<sup>§</sup> Clemens Vonrhein,<sup>⊥</sup> Miguel Teixeira,<sup>§</sup> Manuela M. Pereira,\*<sup>§</sup> and Margarida Archer\*,<sup>§</sup>

<sup>§</sup>Instituto de Tecnologia Química e Biológica, Universidade Nova de Lisboa, Av. da República EAN, 2780-157 Oeiras, Portugal, and

<sup>⊥</sup>Global Phasing Ltd., Sheraton House, Castle Park, Cambridge CB3 0AX, United Kingdom <sup>||</sup>Equally contributing authors

\*Present address: European Synchrotron Radiation Facility, 6 Rue Jules Horowitz, 38043 Grenoble, France

Received March 6, 2009; Revised Manuscript Received May 13, 2009

**ABSTRACT:** A sulfide:quinone oxidoreductase (SQR) was isolated from the membranes of the hyperthermophilic archaeon *Acidianus ambivalens*, and its X-ray structure, the first reported for an SQR, was determined to 2.6 Å resolution. This enzyme was functionally and structurally characterized and was shown to have two redox active sites: a covalently bound FAD and an adjacent pair of cysteine residues. Most interestingly, the X-ray structure revealed the presence of a chain of three sulfur atoms bridging those two cysteine residues. The possible implications of this observation in the catalytic mechanism for sulfide oxidation are discussed, and the role of SQR in the sulfur dependent bioenergetics of *A. ambivalens*, linked to oxygen reduction, is addressed.

Hydrogen sulfide was discovered by Carl Wilhelm Scheele in 1777 (1). It is considered a very toxic substance for aerobic organisms hampering oxygen transport and inhibiting oxygen reduction by heme:copper oxygen reductases, thus preventing energy production by oxidative phosphorylation. Furthermore, sulfide is a strong nucleophile and may react with disulfide bridges and bind to metal centers. Despite its toxicity, which is 5-fold higher than that for carbon monoxide, hydrogen sulfide is a fundamental molecule in both aerobic and anaerobic organisms. H<sub>2</sub>S has now been proposed to be the third signaling “gas” in eukaryotes (2), being of vital importance in the brain, heart, and smooth muscle (3). In mammalian cells the presence of hydrogen sulfide results mainly from the activity of two enzymes, cystathionine  $\gamma$ -lyase (CSE) and cystathionine  $\beta$ -synthetase (CBS) (4). Also, hydrogen sulfide is a metabolite produced by archaea and bacteria present in the lumen of the large intestine. Oxidation of sulfide by animal mitochondria has been demonstrated more than 20 years ago (5), which was shown to be associated with the respiratory chain and coupled to ATP production (6); recently, sulfide has been reported to be the first inorganic substrate of human cells (7).

In archaea and bacteria, H<sub>2</sub>S may be an electron donor to the respiratory chain. Two enzymatic systems are known to be involved in sulfide oxidation: flavocytochrome c (FCC)<sup>1</sup> and sulfide:quinone oxidoreductase (SQR) (8). Genes coding for the latter are present in mitochondrial genomes, including the human one, and a bacterial origin of eukaryotic SQR has been proposed (9). Both of those enzymes are members of the flavin disulfide reductases (FDR) family, which includes glutathione and thioredoxin reductases and dihydrolipoamide dehydrogenases. Members of this family are characterized by having two redox centers, one of these being a FAD. The other redox center, located close to the flavin, can be a pair of cysteine residues, a cysteine-sulfenic acid, or a mixed Cys–S–S–CoA disulfide. In the case of a redox pair of cysteine residues, the sequence position of these residues may vary but is conserved within each subfamily (10).

*Acidianus ambivalens* is a thermoacidophilic archaeon of the *Sulfolobales* order which grows optimally at 85 °C and pH 2 (11, 12). Under aerobic conditions, it uses inorganic sulfur as the energy source, oxidizing it to H<sub>2</sub>SO<sub>4</sub>. Several enzymes involved in its sulfur metabolism and aerobic respiratory chain have been characterized, namely, a heme:copper oxygen reductase (12), a thiosulfate:quinone oxidoreductase (13), and a sulfur oxygenase reductase (SOR), of which sulfide is one of the products (14).

Herein we report a detailed functional and structural characterization of the sulfide:quinone oxidoreductase (SQR) isolated from the membranes of *A. ambivalens*. We have initially crystallized a truncated form of SQR (proteolytically cleaved at the C-terminus) (13), first assigned as a type II NADH dehydrogenase due to its NADH oxidase activity (13). Recently, the complete form of SQR was obtained, which showed exclusively sulfide:quinone oxidoreductase and no NADH dehydrogenase

<sup>†</sup>This work was supported by FCT grants (PTDC/BIA-PRO/66833/2006 to M.A., QUI/59824/2004, BIA-PRO/66557/2006 to M.M.P.). J.A.B. and F.L.S. are recipients of FCT fellowships BD/30512/2006 and BD/27972/2006, respectively.

<sup>‡</sup>The coordinates and structure factors have been deposited in the Protein Data Bank (PDB ID codes: 3H8L for SQR and 3H8I for SQR-T).

<sup>\*</sup>To whom correspondence should be addressed. Telephone: +351214469762/321. Fax: +351214433644/314. E-mail: archer@itqb.unl.pt (M.A.); mpereira@itqb.unl.pt (M.M.P.).

<sup>1</sup>Abbreviations: SQR, sulfide:quinone oxidoreductase; FDRs, flavoprotein disulfide reductases; FCC, flavocytochrome c; HQNO, 2-heptyl-4-hydroxyquinolone N-oxide; DDM, n-dodecyl  $\beta$ -D-maltoside.

activity. The three-dimensional structures of the truncated ( $\text{SQR}_T$ ) and complete (SQR) forms of sulfide:quinone oxidoreductase were determined to 2.7 and 2.6 Å resolution, respectively. Both structures revealed a covalently bound FAD and a pair of adjacent cysteine residues bridged by a chain of three sulfur atoms. A possible sulfide oxidizing mechanism is proposed, and the role of SQR in the global sulfur-linked bioenergetics of *A. ambivalens* is discussed, showing how this enzyme allows *A. ambivalens* to obtain maximal energy from sulfur.

## EXPERIMENTAL PROCEDURES

**Protein Purification.** A truncated form of SQR ( $\text{SQR}_T$ ), lacking ~50 amino acid residues in the C-terminal region, was purified as previously described (15, 16). This enzyme was shown to have NADH:quinone oxidoreductase activity and was thus first assigned as a type II NADH dehydrogenase (16). However, the three-dimensional structure of this form prompted a new functional characterization, which led to the conclusion that it is in fact a sulfide:quinone oxidoreductase. The complete form of SQR (SQR) was then purified by similar procedures, but in the presence of a cocktail of protease inhibitors (Complete Protease inhibitor cocktail tablets from Roche) and by monitoring the sulfide:quinone oxidoreductase activity. To ensure homogeneity of the purified enzyme, mass spectrometry, N-terminal sequencing (performed by ITQB services), and SDS-PAGE (17) were carried out. Protein concentration was determined using the BCA method (18). Flavin extraction was attempted by incubating the protein with 10% trichloroacetic acid as in ref (19). Caldariella quinone, the microorganism's native quinone, was extracted from lyophilized *A. ambivalens* membranes using a (1:1) mixture of chloroform/methanol (20).

**Spectroscopic Characterization.** Electronic spectra were obtained on a Shimadzu UV1603 spectrophotometer at room temperature. Unless stated otherwise, the sample was buffered in 50 mM potassium phosphate, pH 6.5, and 0.1% (w/v) *n*-dodecyl β-D-maltoside (DDM).

**Molecular Mass Determination.** The protein molecular mass determination by gel permeation chromatography was performed in a 24 mL bed volume Superdex S200 column (GE Healthcare), using both high and low molecular mass protein standards (67–669 and 14.4–97 kDa (GE Healthcare)). Elution was made with 40 mM potassium phosphate buffer at pH 6.5, 150 mM NaCl, and 0.1% DDM. For mass spectrometry analysis, *A. ambivalens* SQR with a concentration between 460 and 830 μM was diluted 1:10 in a matrix (sinapinic acid in 70% acetonitrile, 0.1% TFA) and subjected to MALDI-TOF analysis (PO 07MS spectrometer) at the ITQB mass spectrometry facility.

**Sequence Analysis.** Amino acid sequences of enzymes from other organisms were compared using BLAST at NCBI databases. Multiple sequence alignments were produced as previously described (21) and manually adjusted. Dendograms were built with the Geneious software (22).

**Catalytic Activity Assays.** Sulfide oxidase activity in *A. ambivalens* membranes was monitored at 50 °C by measuring O<sub>2</sub> consumption polarographically with a Clark-type oxygen electrode, YSI model 5300 (Yellow Springs). The reaction mixture contained 40 mM potassium phosphate buffer at pH 6.5 and 300 μM Na<sub>2</sub>S (freshly prepared). For NADH consumption assays, 0.3–4.6 mM NADH was used instead of Na<sub>2</sub>S. The reactions were started by the addition of membranes (approximately 210 μg of protein·mL<sup>-1</sup>). For inhibition experiments,

30 mM iodoacetamide (in the same buffer) and an ethanolic solution of HQNO (50 mM) were used (final concentration in the assay of 300 and 500 μM, respectively).

Sulfide:quinone oxidoreductase activity was measured under anaerobic conditions at 50 °C in an Olis DW2 UV/vis spectrophotometer by sulfide-dependent quinone reduction using two beams at the following wavelengths: decylubiquinone, 275–300 nm ( $\Delta\epsilon = 12500 \text{ M}^{-1} \text{ cm}^{-1}$ ); 2,3-dimethyl-1,4-naphthoquinone, 270–290 nm ( $\Delta\epsilon = 15200 \text{ M}^{-1} \text{ cm}^{-1}$ ); 2-methyl-1,4-naphthoquinone (menadione), 280–260 nm ( $\Delta\epsilon = 7800 \text{ M}^{-1} \text{ cm}^{-1}$ ); caldariella quinone, 351–341 nm ( $\Delta\epsilon = 1180 \text{ M}^{-1} \text{ cm}^{-1}$ ). The reaction mixture contained 50 mM potassium phosphate, pH 6.5, 20 mM glucose, 1 unit of glucose oxidase mL<sup>-1</sup>, 10 units of catalase mL<sup>-1</sup>, 0.025% DDM, 50 μM of quinone, and 5–14 μg of protein·mL<sup>-1</sup>. The enzymatic reactions were started by addition of Na<sub>2</sub>S. Inhibition experiments were performed by adding HQNO or KCN (final concentration 100 μM prepared in 200 mM potassium phosphate buffer, pH 6.5) after the addition of Na<sub>2</sub>S. In the case of iodoacetamide, the substrate was added after prior incubation with the inhibitor. Controls were performed in the absence of the enzyme.

The pH activity profile was performed between pH 3 and pH 8 using the following buffers (all at 50 mM concentration with 0.025% DDM): potassium phosphate, pH 3, formic acid between pH 3.5 and pH 4.5, potassium acetate between pH 5 and pH 5.5, and MES/Bis-tris propane between pH 6 and pH 8. In the temperature activity profile, the solution temperature was monitored using a HIBOK 14 thermometer inside the reference cell. NADH:quinone oxidoreductase activity was monitored in the same conditions by following the decrease in absorbance of NADH (initial concentration of 260 μM) at 339 nm.

**Crystallization and X-ray Data.** The crystallization of  $\text{SQR}_T$  using the hanging-drop vapor diffusion method is described in ref (15). In summary, yellow hexagonally shaped crystals were obtained at 20 °C by mixing equal volumes of protein and reservoir solutions containing 2.2 M NH<sub>4</sub>H<sub>2</sub>PO<sub>4</sub> and 100 mM Tris-HCl, pH 8.5 (final pH of the solution was 4.5), or 2.2 M NH<sub>4</sub>H<sub>2</sub>PO<sub>4</sub>/K<sub>2</sub>HPO<sub>4</sub> at pH 4.5. Suitable cryoprotectant conditions were obtained by lowering the precipitant concentration to 1.5 M and adding 25% glycerol. SQR crystallized under similar experimental conditions as the truncated form showing the same crystal morphology. SQR was used at a concentration of ~10 mg·mL<sup>-1</sup> in 10 mM potassium phosphate buffer, pH 6.5, and 0.025% DDM. Crystals were flash-cooled using glycerol as cryoprotectant as aforementioned. X-ray diffraction data were collected from single crystals at liquid nitrogen temperature (100 K). The intensity data were measured on beamline ID14-1 at ESRF (European Synchrotron Radiation Facility, Grenoble) using an ADSC Q210 CCD detector. Data integration and scaling were done with XDS (23) and SCALA (24) from the CCP4 suite of programs (25).

**Structure Determination and Refinement.** The  $\text{SQR}_T$  structure was determined by single isomorphous replacement with anomalous scattering (SIRAS) using a KI derivative as previously described (15). Since crystals of SQR were isomorphous with  $\text{SQR}_T$ , an initial rigid body refinement was done with REFMAC5 (26). Iterative model building and crystallographic refinement were performed with the programs Coot (27) and BUSTER-TNT (28). All structural figures were drawn using PyMOL (29), and the topology diagram was generated by the program Tops (30).

## RESULTS AND DISCUSSION

**Evidence for the Presence of a Sulfide:Quinone Oxidoreductase in *A. ambivalens* Membranes.** *A. ambivalens* membranes were shown to consume O<sub>2</sub> upon addition of Na<sub>2</sub>S at 150 nmol of O<sub>2</sub>·mg<sup>-1</sup>·min<sup>-1</sup>, which implies the presence of a sulfide oxidation system linked to the aerobic respiratory chain. Upon addition of HQNO, a quinone competitive inhibitor, the rate of O<sub>2</sub> consumption decreased by ~80%, while prior incubation with iodoacetamide (alkylating sulphydryl reagent known to bind to cysteine residues) completely abolished O<sub>2</sub> consumption.

**Primary Structure and Sequence Comparison.** Genes encoding SQRs are present in the three domains of life. On the basis of amino acid sequence comparisons, Theissen et al. (9) proposed that SQRs are divided into three groups: group I comprises enzymes from bacteria; group II includes enzymes from bacteria and eukaryotes; group III contains bacterial and archaeal enzymes. With the larger number of sequences now available, a new sequence alignment was performed, whose derived dendrogram (Figure 1) reveals that SQR from *A. ambivalens* and other related archaea cluster in a branch included in group I, and not in group III as would be expected from that classification. Moreover, some archaea have genes encoding several SQRs, belonging either to group I or group III, meaning that the distribution of SQRs is not related to the microbial phyla and evidencing the occurrence of lateral gene transfers throughout evolution of this enzyme family.

The amino acid sequence of the *A. ambivalens* SQR is 13–89% identical to those of other SQRs, which show among themselves a quite low sequence identity. The most similar sequences to the *A. ambivalens* SQR are those from archaea of the same phylogenetic order, the Sulfobolales (Supporting Information Figure S1).

The primary structures of the FDR enzymes have two glycine residue patterns that are part of two Rossmann folds, generally described as the FAD and the NAD(P)H binding domains. Depending on the subfamily, the position of the active cysteine residues can vary, but these positions are conserved within each subfamily (10). As for SQRs, the *A. ambivalens* enzyme has the conserved glycine residue pattern typical of the Rossmann fold near the N-terminus and has two conserved cysteine residues which form a redox active disulfide bridge (8). The presence of the Rossmann fold at the N-terminus and the amino acid sequence position of the conserved cysteine residues compose the fingerprint of the SQR family. In contrast to other FDRs, whose second glycol pattern is part of the second Rossmann fold involved in NAD(P)H binding, SQRs contain an insertion which blocks the NAD(P)H access to the flavin cofactor as shown in the structure described here (Supporting Information Figure S1). Apart from the amino acid residues from these motifs, few other residues are conserved. Among those are (numbering refers to *A. ambivalens* SQR) a highly conserved serine residue (S<sub>127</sub>), a lysine residue (K<sub>315</sub>), and a motif [K<sub>386</sub>-(X)<sub>4–7</sub>-(Y/F)-(X)<sub>0–1</sub>-(Y/W/F)], near the C-terminus. The third cysteine residue (C<sub>129</sub>) that was proposed to participate in the sulfide oxidation mechanism (31), although present in many SQRs from group II, is only strictly conserved in group I enzymes. A glutamic residue, E<sub>184</sub> (E<sub>165</sub> in *Rhodobacter capsulatus* SQR), suggested to act as an active base during catalysis (31) is not strictly conserved and may be substituted by a lysine. There is also an aspartic residue, D<sub>353</sub>, strictly conserved among group I SQRs, lying 3–9 residues downstream of the last conserved cysteine (C<sub>350</sub>). In *R. capsulatus* SQR (8), two histidines (H<sub>131</sub> and H<sub>196</sub>, *R. capsulatus* numbering)

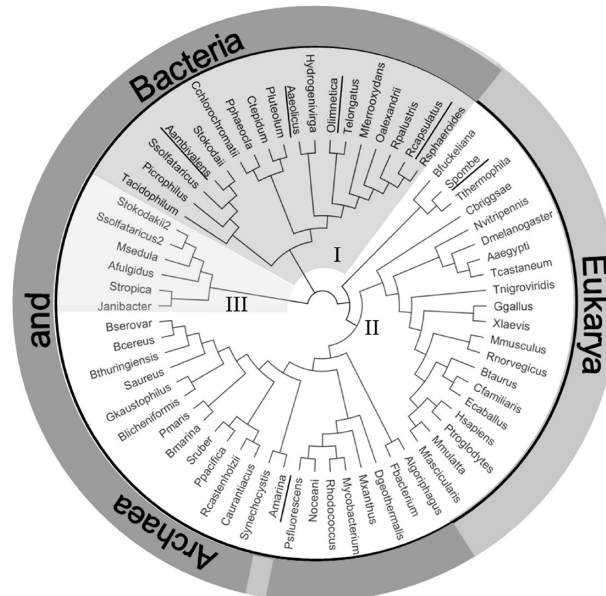


FIGURE 1: Dendrogram of amino acid sequences from SQRs built with the Geneious software. Sequences belonging to groups I, II, and III are indicated by different shadowing. Eukaryote and bacteria and archaea SQRs are indicated at the periphery of the dendrogram. Underlined species names indicate those from which SQRs have been characterized.

were proposed to be involved in quinone binding, but none of these are fully conserved among SQRs.

**Biochemical Characterization.** An SQR was isolated from the membranes of *A. ambivalens*. Up to now seven SQRs have been preliminarily characterized, but only one, from *R. capsulatus*, was more extensively characterized (31–37). The *A. ambivalens* SQR was initially purified in a truncated form, and later a complete form was isolated. The C-terminally truncated form of the enzyme (named SQR-T) of ~40 kDa, has NADH:quinone oxidoreductase activity and was initially considered to be a type II NADH dehydrogenase (16). The complete form of SQR consists of 409 amino acid residues (calculated mass of 45151.85 Da) and has exclusively sulfide:quinone oxidoreductase activity.

SQR was purified to homogeneity as judged both by SDS-PAGE and MALDI-TOF mass spectrometry (data not shown). The oligomerization state of the protein was investigated by gel permeation chromatography, and a single peak corresponding to a molecular mass of ~48 kDa was observed, which indicates that the protein is a monomer in solution under the conditions tested. The electronic absorption spectrum of the as purified SQR has the typical fingerprints of a flavoprotein ( $\lambda_{\text{max}}$  at 454 and 350 nm) (Figure 2a). All attempts to extract the flavin cofactor were unsuccessful as described previously (38), indicating the presence of a covalently bound flavin, now confirmed by the X-ray structure. The structure described here also showed that the flavin cofactor is a flavin adenine dinucleotide (FAD).

**Functional Characterization.** The intact form of the enzyme has exclusively sulfide:quinone oxidoreductase activity with turnovers and specific activities presented in Table 1. The highest sulfide:quinone oxidoreductase activity was observed with the native caldariella quinone, and the reactivity of SQR with quinones seems to be correlated with their reduction potentials: activity increases with the increase of the quinone's reduction potential (Table 1). With decylubiquinone a maximum turnover

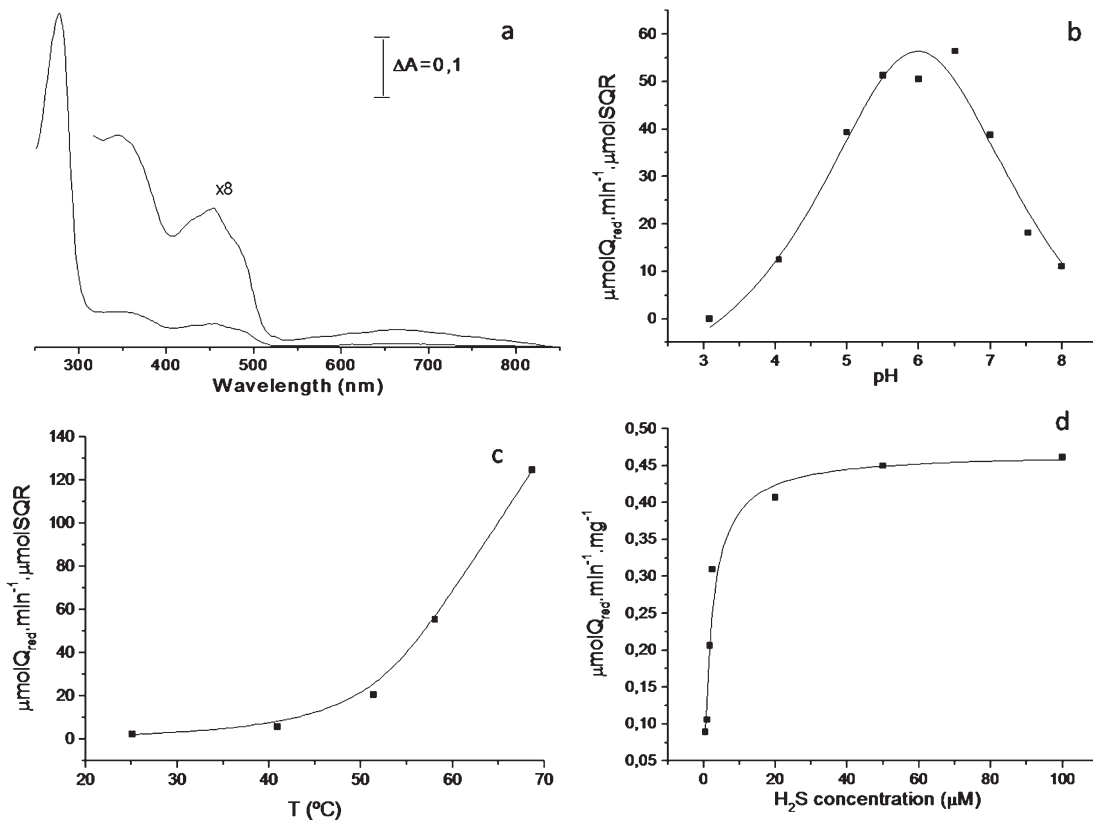


FIGURE 2: (a) UV-visible spectrum of the *A. ambivalens* SQR at pH 6.5. (b) pH (at 50 °C) and (c) temperature (at pH 6.5) profiles of SQR activity using decylubiquinone as substrate. In (b) and (c) lines depicted in the figure are for better visualization. (d) Michaelis–Menten hyperbola using sulfide as substrate (the solid curve was calculated with the parameters presented in the text).

Table 1: Sulfide:Quinone Oxidoreductase Activity of SQR at 50 °C, pH 6.5, with Different Quinones

quinone	specific activity (μmol of quinone reduced · mg⁻¹ · min⁻¹)	turnover (min⁻¹)	redox potential (mV)
2,3-dimethyl-1, 4-naphthoquinone	0.127	6	-60
2-methyl-1, 4-naphthoquinone	0.194	9	0
decylubiquinone	0.470	23	+100
caldariella quinone	0.531	26	+100

of 125 min<sup>-1</sup> was obtained at 70 °C, pH 6.5 (Figure 2b,c). Assays at higher temperatures were not possible to perform due to quinone instability. At 25 °C, only 3% of the activity is detected, indicating that at room temperature the enzyme is almost inactive, as frequently observed for enzymes from hyperthermophiles. The turnover for this enzyme is similar to the one from *Oscillatoria limnetica* (94 min<sup>-1</sup>) (33). At 50 °C, the  $K_m$  and  $V_{max}$  for sulfide were determined to be 2 μM and 0.470 μmol min<sup>-1</sup> mg<sup>-1</sup>, respectively, by monitoring quinol formation (Figure 2d). Reduction of decylubiquinone is 55% inhibited by the quinone analogue HQNO, indicating that quinone reduction is specific. To investigate the possible involvement of the cysteine residues in the oxidation of sulfide, activity assays were performed in the presence of iodoacetamide. Prior incubation of SQR with iodoacetamide led to a complete inhibition of the sulfide-dependent quinone reduction, which suggests that the cysteine residues have indeed an active role in catalysis. The reaction is also inhibited by KCN to 42%, as found for some other SQRs (8).

In the case of SQR<sub>T</sub>, the truncated form of SQR, both NADH and sulfide:quinone oxidoreductase activities are observed, whereas the intact enzyme does not react with NADH. Both SQR and SQR<sub>T</sub> structures have an extra loop blocking the NADH access to the flavin cofactor (see below). This means that the NADH oxidase activity of SQR<sub>T</sub> results from a nonphysiological exposure of the FAD in the truncated enzyme. This conclusion is reinforced by the observations that *A. ambivalens*' membranes consume O<sub>2</sub> upon addition of H<sub>2</sub>S (see above) and that O<sub>2</sub> consumption using NADH as electron donor is negligible. These data indicate that the truncated form is not present in the membranes. NADH and sulfide:quinone oxidoreductase activities were also assayed in the presence of iodoacetamide. As expected, iodoacetamide completely abolished the sulfide-dependent quinone reduction but had no effect on NADH:quinone oxidoreduction.

**Structural Characterization. Crystallographic Refinement and Model Quality.** The complete form of SQR crystallized under similar conditions and is isomorphous to SQR<sub>T</sub>. Crystals appeared within 2 weeks and grew up to maximum dimensions of ~0.2 × 0.15 × 0.1 mm<sup>3</sup>. Crystals belong to the hexagonal space group P6<sub>5</sub>22 with two molecules in the asymmetric unit, unit cell dimensions of  $a = b = 179.7 \text{ \AA}$  and  $c = 163.4 \text{ \AA}$  (for SQR), and contain a high solvent content (~60%).

The SQR<sub>T</sub> X-ray structure was refined to 2.7 Å with an *R*-factor of 19.6% (*R*-free of 22.5%), while the SQR final model shows an *R*-factor of 19.4% (*R*-free of 22.2%) to a resolution of 2.6 Å. X-ray data collection and refinement statistics as well as overall model quality parameters are depicted in Supporting Information Table S1. The electron density maps are of good quality except for two short regions, a bulged β-strand fragment

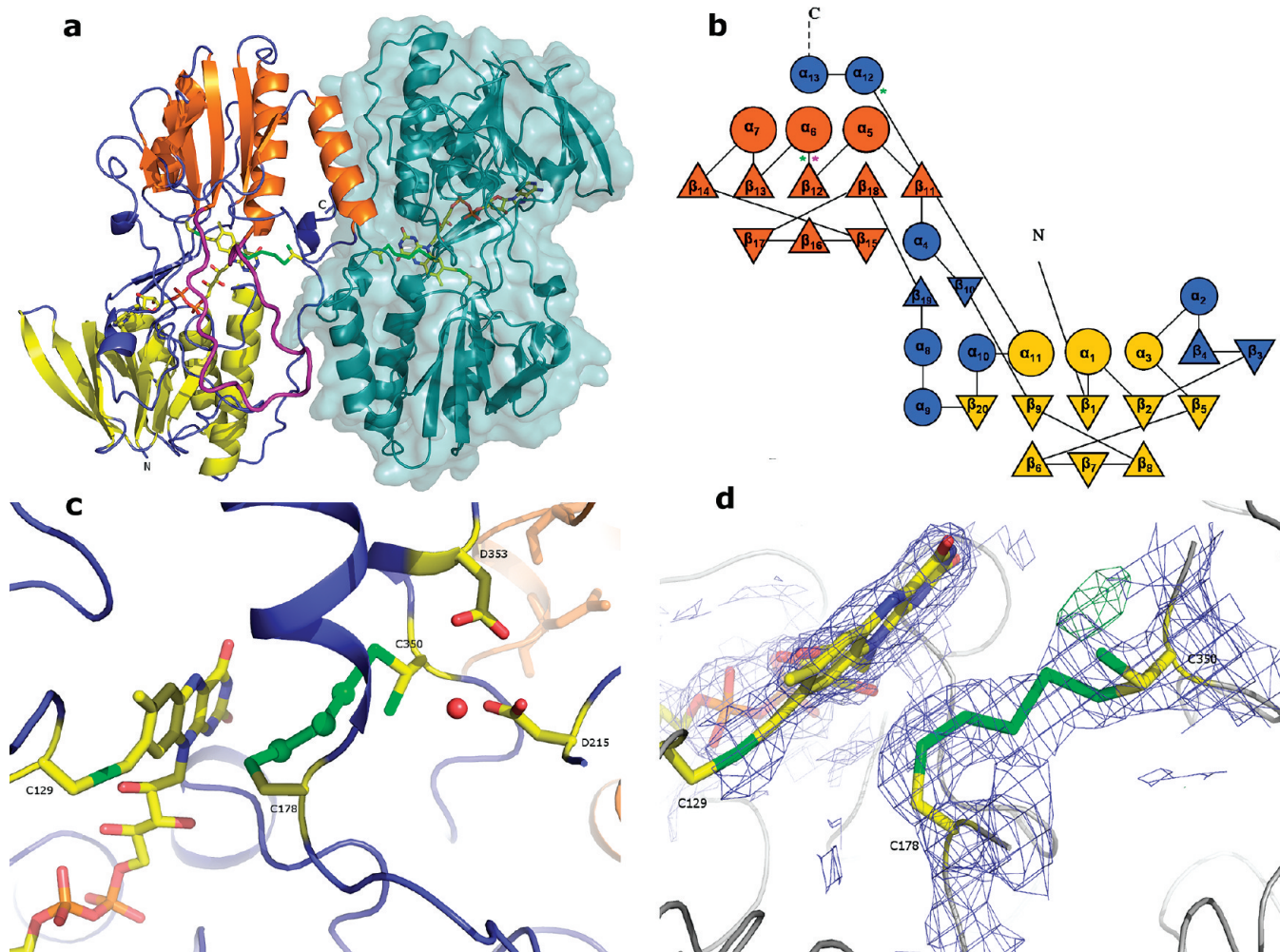


FIGURE 3: (a) Cartoon and surface representation of the crystallographic dimer of SQR. In chain A, the FAD domain is colored in yellow, the second Rossman-like fold domain is in orange, and the loop hindering the access to the second Rossman fold is in purple; chain B is in dark cyan with the molecular surface displayed; in both chains, the FAD, the redox active cysteines, the cysteine covalently binding the FAD, and the trisulfide molecule are shown in sticks. (b) Tops-generated topology diagram of SQR with numbered secondary structure elements ( $\alpha$ -helices in circles and  $\beta$ -sheets in triangles) and numbered; the FAD domain is colored in yellow and the second Rossman-like fold is in orange; the location of the loop blocking the access to the flavin moiety is pointed as a purple asterisk, and the position of the two redox active cysteine residues is pointed as green asterisks. (c) Cartoon representation of SQR redox active sites. FAD and active site residues are shown in stick representation. (d)  $2F_o - F_c$  at  $1.5\sigma$  (blue) and  $F_o - F_c$  at  $5\sigma$  (green) electron density maps around the active site residues (shown in sticks).

(P<sub>43</sub> to A<sub>49</sub>) and an  $\alpha$ -helical stretch (E<sub>130</sub> to A<sub>134</sub>), which show higher thermal motion parameters ( $B$ -factors). No interpretable density was observed for the last 53 amino acid residues at the C-terminal region of the full-length SQR. Hence, similarly to the SQR<sub>T</sub> structure, the crystallographic model of SQR consists of 356 residues per monomer (out of 409). Mass spectrometry analysis of SQR in solution and from dissolved crystals showed that the polypeptide is complete in both samples (data not shown), suggesting high flexibility around the C-terminal region.

**Overall Fold.** The crystal structure of SQR contains two monomers in the asymmetric unit (Figure 3a). The dimer interface is approximately 1500 Å<sup>2</sup> and involves 20 H-bonds and a few hydrophobic contacts suggesting a possible dimeric arrangement of the enzyme in the membranes. Both SQR<sub>T</sub> and SQR structures are very similar, showing an rmsd of 0.14 Å for 356 aligned C<sub>α</sub> atoms (chains A, superposition performed with the “Secondary Structure Matching” tool within Coot (39)). Hereafter, we will refer to the complete SQR structure unless otherwise stated. Each monomer has two domains of similar architecture, which consist of a twisted five-stranded parallel  $\beta$ -sheet flanked by a three-stranded antiparallel  $\beta$ -sheet on one side and by three  $\alpha$ -helices

on the other side, a Rossmann-like fold (see topology diagram, Figure 3b). The presence of these two domains is shared among the enzymes of the FDR family. The first (N-terminal) domain is involved in flavin binding, whereas, in most FDRs, the second domain is involved in NAD(P)H binding, except for SQR and FCC. Flavocytochrome c sulfide dehydrogenase from *Allochromatium vinosum* (FCC) is a heterodimer containing a 46 kDa flavoprotein subunit homologous to FDRs and a 21 kDa diheme cytochrome subunit (PDB code: 1fed) (40). Structural superposition of SQR and FCC flavoprotein subunit yields an rmsd of 2.6 Å for 287 aligned C<sub>α</sub> atoms, where the highest deviations occur in a few loops and at the C-terminus (after N<sub>333</sub>, SQR numbering) (Figure 4).

In contrast to other FDRs, SQR contains an additional 26 amino acid long loop (G<sub>154</sub> to C<sub>178</sub>, loop colored in purple in Figure 3a, Supporting Information Figure S1) inserted in the second Rossmann-like fold, between the first  $\beta$ -strand and  $\alpha$ -helix ( $\beta_{12}$  and  $\alpha_6$ , location of the loop indicated by a purple asterisk in Figure 3b). This loop, with variable length among SQRs, extends toward the FAD binding domain and blocks the NAD(P)H binding cavity present in other FDRs (Supporting

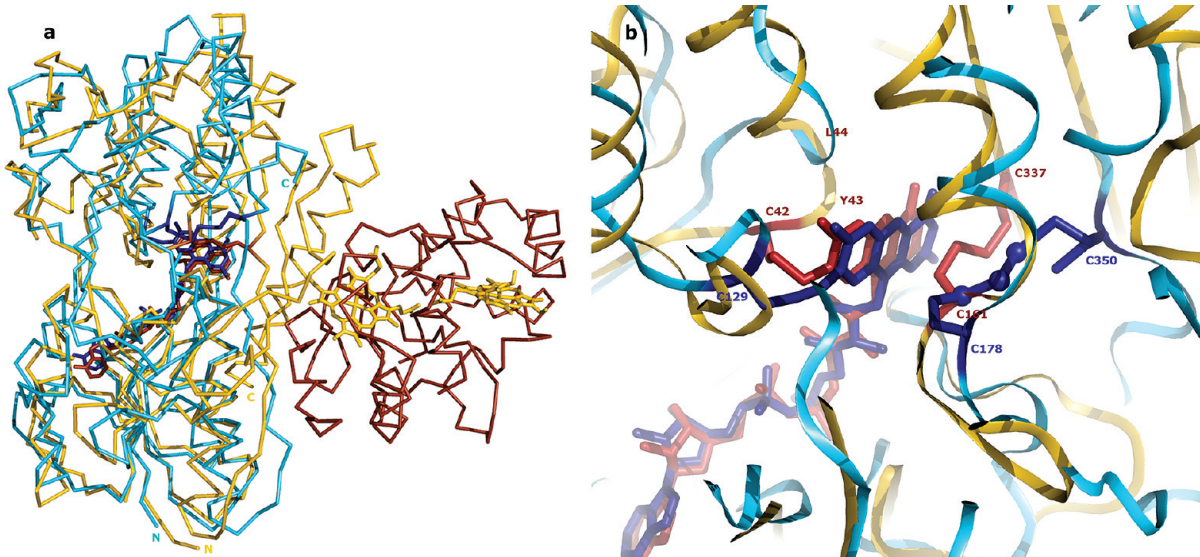


FIGURE 4: (a) Superposition of SQR (cyan) and FCC (yellow) in ribbon representation (chains A) with FADs drawn in sticks (dark blue for SQR and brown for FCC). (b) Close-up view of the active sites, cysteines, and nearby residues close to the *si*-side of flavin in FCC are labeled; the color scheme is as in (a).

Information Figure S1). In FCC, a shorter loop is also observed (heptapeptide segment P<sub>155</sub> to C<sub>161</sub>, FCC numbering). Moreover, in both SQR and FCC the redox pair of cysteine residues is located on the *re*-side of FAD, the same side at which NADH interacts with FAD in most members of the FDR family.

**Redox Active Sites.** The structure of SQR shows two redox active centers, an FAD and an adjacent pair of cysteine residues, C<sub>178</sub> and C<sub>350</sub>, located on the *re*-side of the FAD, of which C<sub>178</sub> is closer to the isoalloxazine ring of FAD (S<sub>y</sub> of C<sub>178</sub> is only 4.1 and 4.8 Å apart from the N<sub>10</sub> and N<sub>5</sub> atoms of FAD, respectively), and the S<sub>y</sub> of C<sub>350</sub> shows two alternate conformations. The FAD is covalently bound to the protein through a thioether bond between the S<sub>y</sub> of C<sub>129</sub> and the 8-methylene group of the isoalloxazine ring (Figure 3c). There are no more contacts between the isoalloxazine ring of FAD and protein amino acid side chains, as also noted for FCC (40). As in these other enzymes, the only noticeable electrostatic interaction that may affect the flavin redox potential and the type of semiquinone formed is the dipole of helix  $\alpha_{11}$  (residues G<sub>317</sub>–L<sub>335</sub>), for which the NH<sub>2</sub> terminus is near N<sub>1</sub> and O<sub>2</sub> of FAD. In FCC, C<sub>161</sub> and C<sub>337</sub> form a disulfide bond, whereas C<sub>42</sub> establishes a covalent linkage with the flavin. The amino acid sequence position of the cysteine residue covalently bound to the flavin and its environment differ significantly in both structures: in SQR, C<sub>129</sub> is located on a turn between strand  $\beta_{11}$  and helix  $\alpha_5$  in the second Rossmann-like fold (NAD(P)H binding domain for most FDRs), whereas C<sub>42</sub> of FCC is situated on a loop between  $\beta_2$  and  $\alpha_2$  of the first Rossmann fold (FAD binding domain) (Figures 3b and 4b). Moreover, in FCC the *si*-face of the flavin ring lies against the polypeptide backbone of residues C<sub>42</sub> to L<sub>44</sub>, in contrast to SQR, where the polypeptide chain is further away, leaving enough free space to accommodate a quinone molecule. Noteworthy in FCC, the electron acceptor is a heme from the cytochrome *c* subunit. The distance between the C<sub>α</sub> atoms of C<sub>178</sub> and C<sub>350</sub> in SQR is ca. 9.3 Å, somewhat larger than the distance of 7.1 Å between the corresponding atoms in FCC. The S<sub>y</sub> atom of C<sub>350</sub> was modeled with two conformations with approximately half-occupancy each in both monomers. Quite remarkably, initial experimental and further difference

Fourier maps consistently revealed continuous electron density between both cysteine residues, which was interpreted as a three sulfur atom chain (denoted S<sub>1</sub>, S<sub>2</sub>, and S<sub>3</sub>) based on geometrical and chemical considerations and further corroborated by anomalous data collected at a longer wavelength (Figure 3c,d and Supporting Information Figure S2). The refined occupancies for the atoms in this trisulfide bridge show a trend of decreasing occupancy from the C<sub>178</sub>-bound S<sub>1</sub> to the C<sub>350</sub>-bound S<sub>3</sub>: 83%/88%/47% in monomer A and 84%/81%/42% in monomer B. This decrease in occupancy relates well to the refined occupancies of the alternate conformations (B) of C<sub>350</sub> to which S<sub>3</sub> is bound. There is an extra spherical blob of electron density in both  $F_o - F_c$  and positive  $F_o - F_c$  maps for both chains (still visible at 6σ in the  $F_o - F_c$  map for chain B), located just above the A conformation of C<sub>350</sub>. This extra density could not be properly modeled, although we think that this blob of density could correspond to an extra sulfur atom, so that this state would represent an intermediate step toward the polysulfide reaction product (see below).

Interestingly, the structure of SQR also revealed the presence of two aspartic residues (D<sub>215</sub> and D<sub>353</sub>) in the vicinity of C<sub>350</sub> (Figure 3c) with a water molecule closely H-bonded to D<sub>215</sub> (~2.6 Å) and further away from D<sub>353</sub> (~3.7 Å), the latter being highly conserved among the SQRs from group I (9). The same water molecule is ca. 5 Å away from the S<sub>y</sub> atoms of C<sub>350</sub> and 5.8 Å from the S<sub>2</sub> atom of the trisulfide molecule.

**Protein Channels.** The molecular surface representation of SQR showed a channel in the protein, at the *re*-side of FAD, which could be the sulfide entry and/or polysulfide exit pathway (Figure 5a). This channel is located between the FAD and the second Rossmann fold domain, has a minimal diameter of ~5 Å, and gives access from the solvent to the catalytic cysteine residues, whereby the most exposed one (C<sub>350</sub>) is approximately 10 Å buried in the protein interior. It is formed mainly by polar and acidic residues, namely, N<sub>173</sub>, S<sub>176</sub>, S<sub>214</sub>, D<sub>175</sub>, D<sub>215</sub>, and E<sub>179</sub>, but also includes P<sub>314</sub> and A<sub>174</sub> and is filled with several ordered water molecules (Figure 5b). Note that the substrate is most probably the neutral, hydrophilic molecule H<sub>2</sub>S, taking into account its pK<sub>a1</sub> of 6.8, and the product a chain of polysulfide or sulfane. It is worth

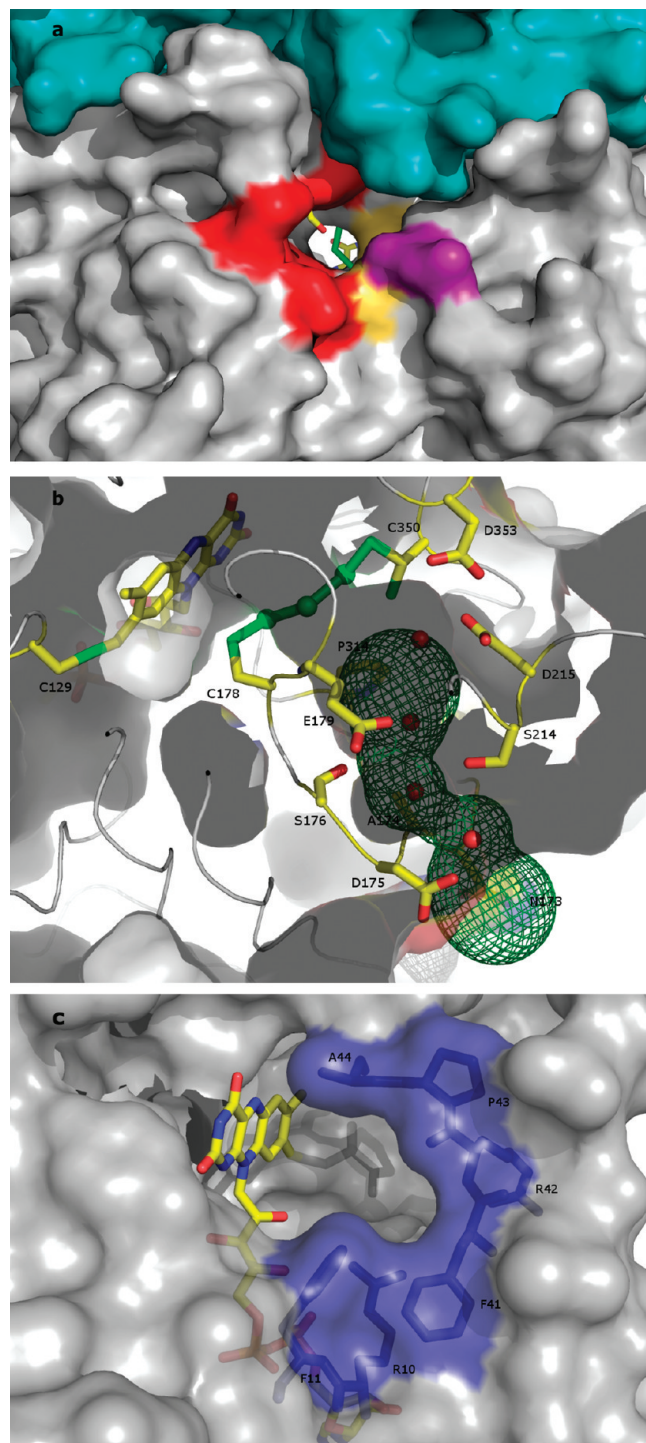


**FIGURE 5:** (a) Molecular surface showing the putative substrate/product channel, with negatively charged residues in red, polar residues in purple, and hydrophobic residues in yellow. S<sub>214</sub> and the sulfur atoms between the redox active cysteine residues are drawn in sticks. Part of chain B is in dark cyan. (b) Surface representation of the channel leading access to the redox active site drawn as a green mesh with relevant residues and water molecules displayed. (c) Quinone binding pocket in surface representation with the relevant hydrophobic residues and FAD displayed in sticks.

mentioning that the optimum pH for the enzyme activity is around 6.

A possible pathway for proton transfer, also located at the *re*-side of FAD, could involve D<sub>307</sub> and K<sub>315</sub>, two conserved residues that form a salt bridge and are connected to the surface through a network of water molecules and some protonatable

groups (H<sub>160</sub> and K<sub>163</sub>). This channel is delimited by the extra loop characteristic of *A. ambivalens* SQR and of some other archaeal enzymes from group I. In *A. vinosum* FCC, a lysine residue (K<sub>303</sub> in FCC numbering) is also located in the same spatial position, in this case, exposed to the solvent.

A possible quinone binding site is the cavity on the *si*-side of FAD (Figure 5c). The cavity is delineated by the backbone of residues F<sub>41</sub> to A<sub>44</sub> (C<sub>α</sub> of A<sub>44</sub> is only ca. 4.7 Å away from N<sub>5</sub> of the isoalloxazine ring) and is flanked by residues R<sub>10</sub>, F<sub>11</sub>, and F<sub>41</sub>; it provides a hydrophobic environment suitable for the quinone head to come close and interact with the isoalloxazine ring of FAD. This cavity, accessible from the protein surface, is located nearby the proposed in-plane amphipathic helix displaying the shortest path to the membrane plane (see below). Worth mentioning, an additional oblong blob of electron density is visible in the 2F<sub>o</sub> – F<sub>c</sub> and positive F<sub>o</sub> – F<sub>c</sub> maps inside the cavity (closest distance is ca. 4.8 Å to N<sub>5</sub> of FAD). Attempts to fit and refine caldariella quinone or a DDM molecule were not satisfactory. The quinone head was pushed away from the plane parallel to the isoalloxazine ring and the detergent molecule's aliphatic tail refined only to low occupancy, so nothing was modeled for this extra blob of density. In FCC, these channels are not observed most probably because the active site is readily accessible to the solvent.

**Membrane Attachment.** SQR was isolated from the membranes of *A. ambivalens*. The structure herein described does not show structural elements that could be involved in membrane binding. However, the model does not contain the last 53 C-terminal residues for which no electron density is visible, even though crystals of the complete form of the protein were obtained. Analysis of the SQR sequence using TMHMM (41) and SOSUI (42) suggested the inexistence of transmembrane helices, but the AmphipathSeek server (43) predicts an amphipathic helix in-plane membrane anchor within the last 25 amino acid residues. Similar results were obtained with the sequences of other SQRs. This kind of membrane anchoring is supposed to occur via a helix with a large hydrophobic region on one side and a hydrophilic one on the other (Supporting Information Figure S3) and has also been observed in other proteins (44, 45). This putative amphipathic helix is most probably located on the *si*-side of the flavin (back of the molecule in relation to Figure 3a).

The location of SQRs in respect to either side of the membrane is still unclear. SQR amino acid sequences do not show typical signal peptides for translocation across the cytoplasmic membrane. However, *R. capsulatus* SQR is suggested to be attached to the periplasmic surface of the cytoplasmic membrane (46).

**Possible Mechanism for Sulfide Oxidation.** Based on the structure here described, a possible mechanism for the oxidation of sulfide is hypothesized, taking into account (i) the involvement of the two cysteine residues C<sub>178</sub> and C<sub>350</sub>, (ii) the presence of the three-sulfur bridge between the two cysteine residues, and (iii) the possible role of acid–base groups either to increase the nucleophilicity of the hydrogen sulfide molecule or to accept, at least transiently, protons. The oxidative part of the reaction occurs on the *re*-side of the flavin, while the reductive part on the *si*-side, where the primary electron acceptor, the quinone, is proposed to bind. At this stage it would be totally speculative to address the reductive cycle, and thus only the oxidation of hydrogen sulfide will be discussed. Also, a three-dimensional representation for the *R. capsulatus* enzyme was modeled (our unpublished data) based on the *A. ambivalens* SQR structure, which reveals that what is here proposed for this enzyme is also possible to occur in the

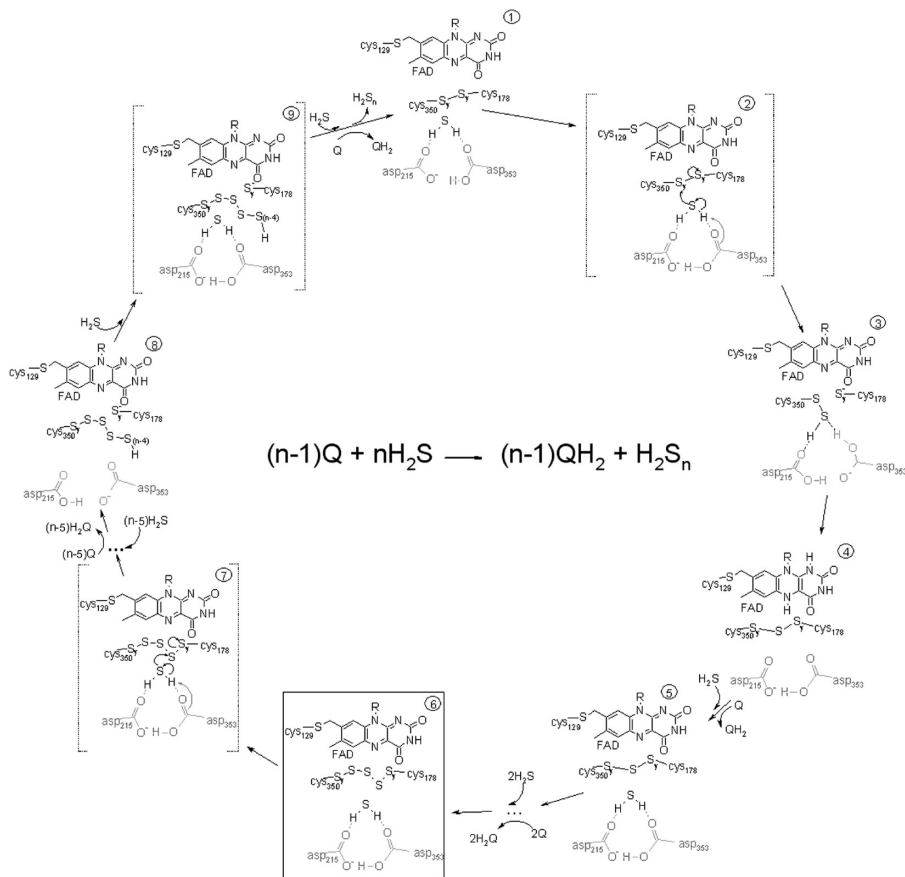


**FIGURE 6:** Schematic representation of the possible mechanism of the *A. ambivalens* SQR reductive half-reaction. (1) represents a possible native state of the enzyme where the FAD, the two redox active cysteine residues, and the two aspartate residues are represented. The  $H_2S$  molecule is stabilized by hydrogen bridges with the oxygens from the aspartyls. The attack of an oxygen atom of one of the aspartic residues to a  $H_2S$  molecule (2) initiates a cascade of nucleophilic attacks that lead to the break of the disulfide bridge and to the formation of a persulfide at  $C_{350}$  and a charge transfer complex with the thiolate of  $C_{178}$  as the donor and the oxidized FAD as the acceptor (states 3 and 8). Then, an active site base abstracts a proton from the persulfide at  $C_{350}$ , a trisulfide bridge is established (4), and the flavin may be reduced. State 5 is formed by the arrival of a new sulfide molecule and after electron transfer from the FAD to the quinone. States equivalent to states 1–5 are repeated until stereochemical constraints hamper the incorporation of another sulfur atom between the cysteine residues. (6) represents the state observed in the structure. From (7) to (9), ( $n - 5$ ) nucleophilic attacks of new sulfide molecules until stereochemical reasons promote the release of the polysulfide molecule from the enzyme and the disulfide bridge is restored (1). Square brackets delimit intermediate stages of the mechanism, and a black square delimits the state observed in the structure herein described.

*R. capsulatus* SQR, including the putative location of the substrate and proton channels, and the quinone binding cavity.

Only two cysteine residues are needed for catalysis: the third cysteine residue ( $C_{129}$ ) is covalently attached to the flavin isoalloxazine ring in *A. ambivalens* SQR and FCC (40); it is too far away from the catalytic site for sulfide oxidation, and, as initially observed by Theissen et al. (9) and now corroborated by the analysis of more SQR amino acid sequences, only two cysteine residues are strictly conserved among all SQRs. The *R. capsulatus* SQR model shows that  $C_{127}$  ( $C_{129}$  in *A. ambivalens* SQR) is certainly involved in the covalent attachment of the FAD. It had also already been mentioned by Griesbeck et al. (31) that eventually only two cysteine residues would be necessary for the catalytic reaction.

In the crystal structure of the as isolated protein, the two reactive cysteine residues are linked with three additional sulfurs in between (Figure 3c,d). Although it cannot be ascertained at the present stage whether this is an intermediate state of the enzyme, it seems reasonable to propose it, as in most other FDRs (namely flavocytochrome *c*) the catalytic cysteine residues form a disulfide bridge in the enzyme's oxidized state (40, 46, 47). Nevertheless, the possible mechanism described below is also compatible if the state observed in the structure is the resting one. In the present

structure, the  $C_\alpha$ 's of  $C_{178}$  and  $C_{350}$  are ca. 9.3 Å apart; however, those residues are located in loop segments, which can accommodate slight conformational changes so that in the oxidized state a simple disulfide bridge may be formed (Figure 6, 1). The first step of the reaction will be the nucleophilic attack (Figure 6, 2) of the incoming substrate  $H_2S$  to the disulfide bridge, being the sulfur incorporated in the nascent polysulfide chain, forming a persulfide at  $C_{350}$  and a thiolate anion at  $C_{178}$  (Figure 6, 3). The nucleophilicity of the hydrogen sulfide molecule may be increased by the involvement of  $D_{215}$  (which is part of the protein channel suggested for substrate conduction) and/or  $D_{353}$ ; this last aspartic residue is highly conserved among SQRs, but  $D_{215}$  is not. However, these residues may be functionally substituted by other amino acid residues: as seen from the amino acid sequence alignments, in SQRs from group I, one of these aspartic residues ( $D_{215}$ ) may be substituted by a histidine residue ( $H_{196}$ , *R. capsulatus* numbering). Mutants of this residue (31) were shown to retain only approximately 40% of the activity of the wild-type enzyme, being the affinity for sulfide decreased, while no change was observed in the  $K_m$  for the quinone. In the *R. capsulatus* SQR homology model the imidazole ring of this histidine residue occupies the same spatial position of the carboxylate group from the aspartic residue. This

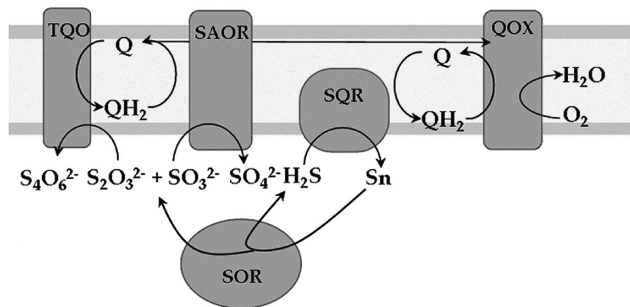


FIGURE 7: Schematic representation of the sulfur energetic metabolism in *A. ambivalens* (TQO, thiosulfate:quinone oxidoreductase; SAOR, sulfite acceptor oxidoreductase; SQR, sulfide:quinone oxidoreductase; QOX, quinol:O<sub>2</sub> oxidoreductase; SOR, sulfur oxygenase reductase).

indicates that although not essential for activity, this residue could be involved in SQR's catalytic cycle.

A charge transfer complex between the C<sub>178</sub> thiolate and FAD<sub>ox</sub> may occur as proposed before (31) (Figure 6, 3). Subsequently, an active site base is suggested to abstract a proton from the persulfide at C<sub>350</sub> to form a more nucleophilic anion. The nature of this base is still unknown, and although it was suggested to be a glutamate residue (E<sub>165</sub> in *R. capsulatus* which corresponds to E<sub>184</sub> in *A. ambivalens*) (31), the present structure shows that it is not within hydrogen-bonding distance of the cysteine residues (S<sub>γ</sub> of C<sub>178</sub> is ca. 8.4 Å apart from O<sub>ε1</sub> of E<sub>184</sub>).

For a trisulfide bridge to be formed, the transfer of two electrons to FAD occurs, possibly through the establishment of covalent adducts with C<sub>178</sub>. A flavin hydroquinone may be formed (Figure 6, 4), which will be subsequently oxidized by the quinone (Figure 6, 5). Incorporation of two more sulfur atoms to the nascent polysulfide gives rise to an intermediate state with three sulfur atoms between the cysteine residues as observed in the structure here described (Figure 6, 6). Stereochemical constraints will determine the maximum number of sulfur atoms to be incorporated: once it is achieved, two consecutive nucleophilic attacks of two new hydrogen sulfide molecules on the trisulfide lead to the release of a polysulfide molecule from the enzyme, and the initial disulfide bridge is restored (Figure 6, 7–9).

The reaction product of sulfide oxidation is not known. If what is observed in the structure of the as purified *A. ambivalens* SQR is an intermediate, then the shortest polysulfide/sulfane product should be S<sub>5</sub><sup>2-</sup> or S<sub>5</sub>H<sub>2</sub>. In fact, it has been shown that at pH 6 the most stable form of polysulfide comprises four or five sulfur atoms (47), which can be further substrates to sulfur oxygenase reductase (SOR).

**SQR in *A. ambivalens*, the Link between Sulfur Metabolism and the Aerobic Respiratory Chain.** In aerobically grown *A. ambivalens* the initial step of sulfur metabolism is mediated by a soluble SOR. This enzyme catalyzes the disproportionation of S<sup>0</sup> to sulfite, sulfide, and possibly thiosulfate. In this way, not all energy from sulfur is used, since part of it is lost in sulfur reduction to sulfide. However, this energy is recovered by the presence of SQR, which oxidizes sulfide (producing polysulfides/sulfanes that are again substrates for SOR) and reduces quinones. Thus, this process allows to extract maximum energy from S<sup>0</sup>, feeding electrons to the respiratory chain.

The products of sulfur oxidation, sulfite and thiosulfate, are also further metabolized. There is evidence for the existence of a sulfite:acceptor oxidoreductase (SAOR) in the membranes of *A.*

*ambivalens*, although the enzyme has never been isolated (48), and a membrane-bound thiosulfate:quinone oxidoreductase (TQO) has been purified and characterized (13). In this way, SOR and SQR create an energetic spiral, allowing to get the maximum of energy from sulfur compounds (Figure 7), and ultimately, the SOR/SQR/TQO/SAOR enzymes enable a full utilization of sulfur for energy conservation in *A. ambivalens* with three direct links of sulfur oxidation to quinone reduction as the main electron carrier to the quinol:oxygen oxidoreductase, the aa<sub>3</sub> enzyme.

## ACKNOWLEDGMENT

The authors thank Pedro Matias and Carlos Frazão for help with synchrotron data collection, Bruno Victor for the modeling of *R. capsulatus* SQR, Cláudio M. Soares for helpful discussions, and Inês A. C. Pereira for critical reading of the manuscript. We also acknowledge Elizabete Pires and Gonçalo da Costa from the Mass Spectrometry Service at Instituto de Tecnologia Química e Biológica, Universidade Nova de Lisboa, Oeiras, Portugal.

## SUPPORTING INFORMATION AVAILABLE

X-ray diffraction data collection and refinement statistics (Table S1), amino acid sequence alignment of *A. ambivalens* SQR with sulfide:quinone oxidoreductases from group I (Figure S1), anomalous difference Fourier map showing the continuous electron density bridging the two redox active site cysteine residues (Figure S2), and the putative amphipathic helix proposed to be involved in membrane attachment at the C-terminus (residues 385–409) (Figure S3). This material is available free of charge via the Internet at <http://pubs.acs.org>.

## REFERENCES

- Dobbin, L. (1931) The Collected Papers of Carl Wilhem Scheele, 1st ed., G. Bell & Sons, York House, London.
- Wang, R. (2002) Two's company, three's a crowd: can H<sub>2</sub>S be the third endogenous gaseous transmitter?. *FASEB J.* 16, 1792–1798.
- Lloyd, D. (2006) Hydrogen sulfide: clandestine microbial messenger?. *Trends Microbiol.* 14, 456–462.
- Qu, K., Lee, S. W., Bian, J. S., Low, C. M., and Wong, P. T. (2008) Hydrogen sulfide: neurochemistry and neurobiology. *Neurochem. Int.* 52, 155–165.
- Powell, M. A., and Somero, G. N. (1986) Hydrogen sulfide oxidation is coupled to oxidative phosphorylation in mitochondria of *Solemya reidi*. *Science* 233, 563–566.
- Ouml, Lkel, S., and Grieshaber, M. (1997) Sulphide oxidation and oxidative phosphorylation in the mitochondria of the lugworm. *J. Exp. Biol.* 200, 83–92.
- Goubern, M., Andriamihaja, M., Nubel, T., Blachier, F., and Bouillaud, F. (2007) Sulfide, the first inorganic substrate for human cells. *FASEB J.* 21, 1699–1706.
- Griesbeck, C., Hauska, G., and Schutz, M. (2000) Biological Sulfide Oxidation: Sulfide:Quinone-Reductase (SQR), the Primary Reaction, Vol. 4, Research Signpost, Trivandrum, India.
- Theissen, U., Hoffmeister, M., Grieshaber, M., and Martin, W. (2003) Single eubacterial origin of eukaryotic sulfide:quinone oxidoreductase, a mitochondrial enzyme conserved from the early evolution of eukaryotes during anoxic and sulfidic times. *Mol. Biol. Evol.* 20, 1564–1574.
- Argyrou, A., and Blanchard, J. S. (2004) Flavoprotein disulfide reductases: advances in chemistry and function. *Prog. Nucleic Acid Res. Mol. Biol.* 78, 89–142.
- Zillig, W., Yeats, S., Holz, I., Rettenberger, M., Gropp, F., and Simon, G. (1986) *Desulfurobacter ambivalens*, gen. nov., sp. nov., an autotrophic archaeabacterium facultatively oxidizing or reducing sulfur. *Syst. Appl. Microbiol.* 8, 197–203.
- Gomes, C. M., Backgren, C., Teixeira, M., Puustinen, A., Verkhovskaya, M. L., Wikstrom, M., and Verkhovsky, M. I. (2001) Heme-copper oxidases with modified D- and K-pathways are yet efficient proton pumps. *FEBS Lett.* 497, 159–164.
- Muller, F. H., Bandeiras, T. M., Urich, T., Teixeira, M., Gomes, C. M., and Kletzin, A. (2004) Coupling of the pathway of sulphur

- oxidation to dioxygen reduction: characterization of a novel membrane-bound thiosulphate:quinone oxidoreductase. *Mol. Microbiol.* 53, 1147–1160.
14. Urich, T., Bandeiras, T. M., Leal, S. S., Rachel, R., Albrecht, T., Zimmermann, P., Scholz, C., Teixeira, M., Gomes, C. M., and Kletzin, A. (2004) The sulphur oxygenase reductase from *Acidianus ambivalens* is a multimeric protein containing a low-potential mononuclear non-haem iron centre. *Biochem. J.* 381, 137–146.
  15. Brito, J. A., Bandeiras, T. M., Teixeira, M., Vonrhein, C., and Archer, M. (2006) Crystallisation and preliminary structure determination of a NADH:quinone oxidoreductase from the extremophile *Acidianus ambivalens*. *Biochim. Biophys. Acta* 1764, 842–845.
  16. Gomes, C. M., Bandeiras, T. M., and Teixeira, M. (2001) A new type-II NADH dehydrogenase from the archaeon *Acidianus ambivalens*: characterization and in vitro reconstitution of the respiratory chain. *J. Bioenerg. Biomembr.* 33, 1–8.
  17. Laemmli, U. K. (1970) Cleavage of structural proteins during the assembly of the head of bacteriophage T4. *Nature* 227, 680–685.
  18. Smith, P. K., Krohn, R. I., Hermanson, G. T., Mallia, A. K., Gartner, F. H., Provenzano, M. D., Fujimoto, E. K., Goede, N. M., Olson, B. J., and Klenk, D. C. (1985) Measurement of protein using bicinchoninic acid. *Anal. Biochem.* 150, 76–85.
  19. Susin, S., Abian, J., Sanchez-Baeza, F., Peleato, M. L., Abadia, A., Gelpi, E., and Abadia, J. (1993) Riboflavin 3'- and 5'-sulfate, two novel flavins accumulating in the roots of iron-deficient sugar beet (*Beta vulgaris*). *J. Biol. Chem.* 268, 20958–20965.
  20. Hu, H. Y., Fujie, K., and Urano, K. (1999) Development of a novel solid phase extraction method for the analysis of bacterial quinones in activated sludge with a higher reliability. *J. Biosci. Bioeng.* 87, 378–382.
  21. Thompson, J. D., Gibson, T. J., Plewniak, F., Jeanmougin, F., and Higgins, D. G. (1997) The CLUSTAL\_X windows interface: flexible strategies for multiple sequence alignment aided by quality analysis tools. *Nucleic Acids Res.* 25, 4876–4882.
  22. Drummond, A. J., Ashton, B., Cheung, M., Heled, J., Kearse, M., Moir, R., Stones-Havas, S., Thierer, T., and Wilson, A. (2009) Geneious v4.2, Available at <http://www.geneious.com>.
  23. Kabsch, W. (1993) Automatic processing of rotation diffraction data from crystals of initially unknown symmetry and cell constants. *J. Appl. Crystallogr.* 26, 795–800.
  24. Evans, P. R. (1997) *Proceedings of the CCP4 Study Weekend. Recent Advances in Phasing*, 97–102.
  25. Collaborative Computational Project, N. (1994) The CCP4 suite: programs for protein crystallography. *Acta Crystallogr., Sect. D: Biol. Crystallogr.* 50, 760–763.
  26. Murshudov, G. N., Vagin, A. A., and Dodson, E. J. (1997) Refinement of macromolecular structures by the maximum-likelihood method. *Acta Crystallogr., Sect. D: Biol. Crystallogr.* 53, 240–255.
  27. Emsley, P., and Cowtan, K. (2004) Coot: model-building tools for molecular graphics. *Acta Crystallogr., Sect. D: Biol. Crystallogr.* 60, 2126–2132.
  28. Bricogne, G., Blanc, E., Brandl, M., Flensburg, C., Keller, P., Paciorek, W., Roversi, P., Smart, O. S., Vonrhein, C., and Womack, T. (2008). Global Phasing Ltd., Cambridge, UK.
  29. DeLano, W. (2002) DeLano Scientific, San Carlos, CA.
  30. Westhead, D. R., Hatton, D. C., and Thornton, J. M. (1998) An atlas of protein topology cartoons available on the World-Wide Web. *Trends Biochem. Sci.* 23, 35–36.
  31. Griesbeck, C., Schutz, M., Schodl, T., Bathe, S., Nausch, L., Mederer, N., Vielreicher, M., and Hauska, G. (2002) Mechanism of sulfide-quinone reductase investigated using site-directed mutagenesis and sulfur analysis. *Biochemistry* 41, 11552–11565.
  32. Theissen, U., and Martin, W. (2008) Sulfide:quinone oxidoreductase (SQR) from the lugworm *Arenicola marina* shows cyanide- and thioredoxin-dependent activity. *FEBS J.* 275, 1131–1139.
  33. Arieli, B., Shahak, Y., Taglicht, D., Hauska, G., and Padan, E. (1994) Purification and characterization of sulfide-quinone reductase, a novel enzyme driving anoxygenic photosynthesis in *Oscillatoria linnetica*. *J. Biol. Chem.* 269, 5705–5711.
  34. Shibata, H., and Kobayashi, S. (2006) Characterization of a HMT2-like enzyme for sulfide oxidation from *Pseudomonas putida*. *Can. J. Microbiol.* 52, 724–730.
  35. Wakai, S., Tsujita, M., Kikumoto, M., Manchur, M. A., Kanao, T., and Kamimura, K. (2007) Purification and characterization of sulfide:quinone oxidoreductase from an acidophilic iron-oxidizing bacterium *Acidithiobacillus ferrooxidans*. *Biosci. Biotechnol. Biochem.* 71, 2735–2742.
  36. Shibata, H., Suzuki, K., and Kobayashi, S. (2007) Menaquinone reduction by an HMT2-like sulfide dehydrogenase from *Bacillus stearothermophilus*. *Can. J. Microbiol.* 53, 1091–1100.
  37. Vande Weghe, J. G., and Ow, D. W. (1999) A fission yeast gene for mitochondrial sulfide oxidation. *J. Biol. Chem.* 274, 13250–13257.
  38. Bandeiras, T. M., Salgueiro, C., Kletzin, A., Gomes, C. M., and Teixeira, M. (2002) *Acidianus ambivalens* type-II NADH dehydrogenase: genetic characterisation and identification of the flavin moiety as FMN. *FEBS Lett.* 531, 273–277.
  39. Krissinel, E., and Henrick, K. (2004) Secondary-structure matching (SSM), a new tool for fast protein structure alignment in three dimensions. *Acta Crystallogr., Sect. D: Biol. Crystallogr.* 60, 2256–2268.
  40. Chen, Z. W., Koh, M., Van Driessche, G., Van Beeumen, J. J., Bartsch, R. G., Meyer, T. E., Cusanovich, M. A., and Mathews, F. S. (1994) The structure of flavocytochrome c sulfide dehydrogenase from a purple phototrophic bacterium. *Science* 266, 430–432.
  41. <http://www.cbs.dtu.dk/services/TMHM/>.
  42. Hirokawa, T., Boon-Chieng, S., and Mitaku, S. (1998) SOSUI: classification and secondary structure prediction system for membrane proteins. *Bioinformatics* 14, 378–379.
  43. Sapay, N., Guermeur, Y., and Deleage, G. (2006) Prediction of amphipathic in-plane membrane anchors in monotopic proteins using a SVM classifier. *BMC Bioinf.* 7, 255.
  44. Nina, M., Berneche, S., and Roux, B. (2000) Anchoring of a monotopic membrane protein: the binding of prostaglandin H2 synthase-1 to the surface of a phospholipid bilayer. *Eur. Biophys. J.* 29, 439–454.
  45. Penin, F., Brass, V., Appel, N., Ramboarina, S., Montserret, R., Ficheux, D., Blum, H. E., Bartenschlager, R., and Moradpour, D. (2004) Structure and function of the membrane anchor domain of hepatitis C virus nonstructural protein 5A. *J. Biol. Chem.* 279, 40835–40843.
  46. Schutz, M., Maldener, I., Griesbeck, C., and Hauska, G. (1999) Sulfide-quinone reductase from *Rhodobacter capsulatus*: requirement for growth, periplasmic localization, and extension of gene sequence analysis. *J. Bacteriol.* 181, 6516–6523.
  47. Giggenbach, W. (1972) Optical spectra and equilibrium distribution of polysulfide ions in aqueous solution at 20 °C. *Inorg. Chem.* 11, 1201–1207.
  48. Kletzin, A., Urich, T., Muller, F., Bandeiras, T. M., and Gomes, C. M. (2004) Dissimilatory oxidation and reduction of elemental sulfur in thermophilic archaea. *J. Bioenerg. Biomembr.* 36, 77–91.